Available online at www.sciencedirect.com
ScienceDirect
ELSEVIER
Nuclear Physics A 837 (2010) 145–162
NUCLEAR PHYSICS A
www.elsevier.com/locate/nuclphysa

Isoscaling of mass A $\simeq$ 40 reconstructed quasiprojectiles from collisions in the Fermi energy regime

S. Galanopoulos [a,1], G.A. Souliotis [a,b,*], A.L. Keksis [a,c,2], M. Veselsky [a,d], Z. Kohley [a,c], L.W. May [a,c], D.V. Shetty [a,3], S.N. Soisson [a,c], B.C. Stein [a,c], S. Wuenschel [a,c], S.J. Yennello [a,c]

[a] *Cyclotron Institute, Texas A&M University, College Station, TX 77843, USA*
[b] *Laboratory of Physical Chemistry, Department of Chemistry, National and Kapodistrian University of Athens, Athens, Greece*
[c] *Chemistry Department, Texas A&M University, College Station, TX 77843, USA*
[d] *Institute of Physics, Slovak Academy of Sciences, Bratislava, Slovakia*

Received 20 September 2009; received in revised form 28 December 2009; accepted 26 January 2010

Available online 23 March 2010

Abstract

Isoscaling studies of fragments with $Z = 1$–8 from reconstructed quasiprojectiles of mass A $\simeq$ 40 from the ^{40}Ar $+^{124}$ Sn, ^{112}Sn and ^{40}Ca $+^{124}$ Sn, ^{112}Sn reactions at beam energy of 45 MeV/nucleon were performed. After initial efforts to obtain isoscaling with the "traditional" approach of using pairs of systems differing in their isospin asymmetry (or neutron-to-proton ratio N/Z), "intra-system" isoscaling for each of these four systems was obtained using fragment sources restricted in two narrow N/Z regions (one neutron-rich and one neutron-poor). The observed isoscaling behavior was excellent and the isoscaling parameter α was found to decrease with increasing excitation energy. Corrections due to undetected neutrons were also taken into account in the source N/Z determination by using the theoretical models DIT (Deep Inelastic Transfer) and SMM (Statistical Multifragmentation Model) along with a software replica of the experimental setup. These corrections were applied to the determination of the parameter Δ (expressing the difference in the isospin asymmetry of the two sources used in the isoscaling). The reduced isoscaling parameter α/Δ

* Corresponding author at: Cyclotron Institute, Texas A&M University, College Station, TX 77843, USA.
E-mail addresses: soulioti@comp.tamu.edu, soulioti@chem.uoa.gr (G.A. Souliotis).

[1] Present address: Greek Army Academy, Department of Physical Sciences, Athens, Greece.
[2] Present address: C-NR, Los Alamos National Laboratory, NM 87545, USA.
[3] Present address: Physics Department, Western Michigan University, Kalamazoo, MI 49008, USA.

0375-9474/$ – see front matter
doi:10.1016/j.nuclphysa.2010.01.248

was obtained and found to decrease as the excitation energy of the quasiprojectile source increases, in good agreement with recent work on reconstructed mass A $\simeq 80$ quasiprojectiles. This decrease of α/Δ may point to a decrease of the symmetry energy coefficient with increasing excitation energy.

Keywords: NUCLEAR REACTIONS ^{112,124}Sn(^{40}Ar,X), (^{40}Ca,X), $E = 45$ MeV/nucleon; measured light fragment yields, energy spectra, (fragment)(fragment)-coin using FAUST array; analyzed isoscaling behavior versus neutron number and excitation energy, including correction for neutron loss

1. Introduction

One of the most important topics of current research in the nuclear physics and astrophysics community is the determination of the nuclear equation of state (EOS) [1–5]. The nuclear EOS determines the relationship between energy, temperature, density and isospin asymmetry for a nuclear system and is traditionally divided into an isospin symmetric contribution ($N \approx Z$) and a symmetry energy part, quadratically dependent on isospin asymmetry. The symmetry energy, expressing the energy difference between symmetric nuclear matter and pure neutron matter, while rather well determined near normal nuclear density, is not adequately constrained away from this density. The symmetry energy plays a fundamental role in a number of astrophysical topics like the structure and cooling of neutron stars and the dynamics of supernova explosions [6–8], as well as in nuclear physics issues most notably the structure of nuclei away from the valley of stability [9–12]. Information on the symmetry energy has been extracted from the neutron skin [9], elastic scattering of neutron rich nuclei [13], as well as from heavy-ion collisions [1,2,4,14,15]. One observable sensitive to the symmetry energy is the fragment isotopic composition investigated using the isoscaling approach [2,16–18]. In the isoscaling which refers to an exponential relation between the yields of a given fragment from two similar reactions which differ only in their isospin asymmetry (or, equivalently, N/Z), the effects of the nuclear symmetry energy are, to a large extent, isolated in the fragment yields ratios, allowing access of the symmetry energy coefficient during the formation of hot fragments [16–25]. In the present work, we investigated the isoscaling of isotopically resolved fragments with $Z = 1$–8 coming from the multifragmentation of hot primary fragments (quasi-projectiles) of the systems ^{40}Ar + ^{124}Sn, ^{112}Sn and ^{40}Ca + ^{124}Sn, ^{112}Sn at 45 MeV/nucleon. The paper is organized as follows. In Section 2, a brief description of the experimental device and analysis approach is given. In Section 3, after a short discussion of quasiprojectile selection, the isoscaling studies are presented in detail. A discussion on interpretation of the results and delineation of future steps is provided in Section 4. Finally, a summary is given in Section 5.

2. Experimental setup

The experimental work was performed at the Cyclotron Institute of Texas A&M University. Beams of ^{40}Ar and ^{40}Ca ions of energy 45 MeV/nucleon were delivered by the K500 superconducting cyclotron and interacted with isotopically enriched ^{124}Sn and ^{112}Sn targets. Fragments produced in peripheral and semi-peripheral collisions were detected by the FAUST multi-detector array [26,27]. The FAUST array consists of 68 ΔE–E (Si–CsI(Tl)) particle telescopes arranged in five rings as schematically shown in Fig. 1. FAUST provides 90% angular coverage from 2.3° to 33.6°, which is ideal for collecting fragments from the breakup of quasiprojectiles coming

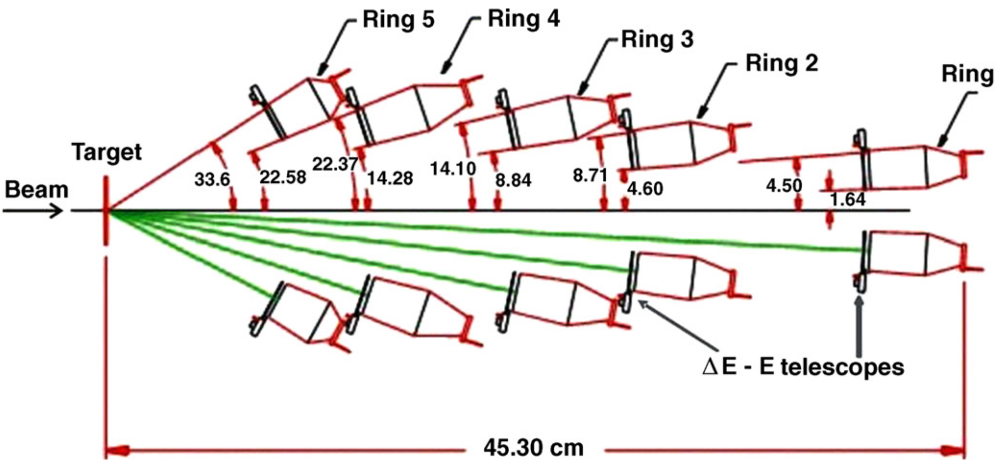

Fig. 1. (Color online.) Schematic drawing of the "FAUST" multidetector array indicating the relative location of the various detector rings [26,28].

from heavy-ion reactions in the Fermi energy regime. The high threshold of the detectors effectively blocks fragments originating from the quasitarget, due to their lower momentum. In the present work, the detector system provided isotopic identification of elements with $Z = 1$–8. FAUST detects the "cold" fragments coming from the de-excitation of the "hot" primary fragments produced in the collisions. The fragment properties directly derived from the experimental apparatus were the atomic number, the mass number, the energies deposited in the Si and CsI detectors and, of course, the detector angles. The details of the calibration procedure and analysis can be found in [28]. Two or more fragments detected in coincidence consisted a reconstructed event. In order to obtain the atomic number Z_{event} and mass number A_{event} of the event, the atomic numbers Z_f and mass numbers A_f, respectively, of all the fragments of the event were summed:

$$Z_{event} = \sum Z_f, \tag{1}$$

$$A_{event} = \sum A_f. \tag{2}$$

The excitation energy E^*_{event} of the reconstructed event was determined from energy balance:

$$E^*_{event} = \sum (m_f + E_{f,cm}) - m_{event}, \tag{3}$$

where m_f and m_{event} are the fragment and the event mass–energy (obtained from standard mass tables), respectively, and $E_{f,cm}$ is the kinetic energy of each fragment in the center of mass system.

3. Analysis and results

3.1. Reconstruction and quasi-projectile selection

As already mentioned, the detection of the fragments is performed by the FAUST detector on an event-by-event basis providing the opportunity to isotopically and kinematically reconstruct the primary fragments. Since FAUST is a charged particle detector array, neutrons cannot be detected. As a result, the reconstructed events may have the correct atomic number, but smaller than the actual mass number, due to this inability to detect neutrons [28].

In the present analysis, quasiprojectiles were selected from the reconstructed events as discussed below. First, to ensure selection of fragments coming from the decay of quasiprojectiles, the parallel velocity component (with respect to the beam direction) of each individual fragment was required to be greater than the velocity of the c.m. of the projectile–target system. The main criterion for QP selection was that the total Z of the reconstructed event be close to the Z of the projectile. More specifically, for the ^{40}Ar + ^{124}Sn, ^{112}Sn systems the Z range chosen was $Z_{QP} = 12$–21, whereas for the ^{40}Ca + ^{124}Sn, ^{112}Sn, the corresponding range was $Z_{QP} = 14$–23. In the upper parts of each panel in Fig. 2, the velocity versus Z_{event} distributions for the reconstructed events are presented. The boxes indicate the Z ranges of quasiprojectiles, as mentioned above. The lower parts of each panel show the Z_{event} distributions (with the Z_{QP} ranges now indicated by horizontal lines). The combination of the reaction kinematics and the detector setup ensure that essentially the criterion on the reconstructed Z_{QP} (be close to the projectile Z) provides an efficient selection of quasiprojectiles. [For completeness, we note that in Fig. 2 (upper parts of each panel) the intense peaks present at $Z_{event} = 5$–7 are due to incomplete reconstruction of the corresponding events.] After the experimental selection of quasiprojectiles for each reaction system, we proceeded to the systematic investigation of the isoscaling behavior of the fragments produced in these reactions.

3.2. Isoscaling studies

As briefly mentioned in the Introduction, the yield ratio $R_{21}(N, Z)$ of a given fragment produced in two similar reactions that differ in their isospin content can exhibit isoscaling which has been observed experimentally [2,16,17,19,20] and obtained in theoretical studies [16–18,21–25] in a variety of reactions. In general, isoscaling, occurring when the two reactions take place at the same temperature and differ only in their isospin asymmetry, is expressed by the relation

$$R_{21}(N, Z) \equiv \frac{Y_2(N, Z)}{Y_1(N, Z)} = C \exp(\alpha N + \beta Z), \tag{4}$$

where $Y_2(N, Z)$ and $Y_1(N, Z)$ are the fragment yields from the neutron rich and the neutron deficient source, respectively, α and β are the scaling parameters and C is an overall normalization factor. (It is common to consider reaction 2 as the neutron rich source, while reaction 1 as the neutron deficient one.) The isoscaling parameter α is related to the symmetry energy coefficient C_{sym} of the nuclear binding energy through the relation [16–18,21–23]

$$\alpha = \frac{4C_{sym}}{T}\left[\left(\frac{Z}{A}\right)_1^2 - \left(\frac{Z}{A}\right)_2^2\right] \equiv \frac{4C_{sym}}{T}\Delta, \tag{5}$$

where Z_1, Z_2 and A_1, A_2 are the charge and mass numbers of the sources from the two systems, respectively, and T their common temperature. This relation provides a valuable link between the measurable quantities and the nuclear symmetry energy coefficient. It should be pointed out that the parameter α refers to the hot primary fragments which undergo sequential decay into cold secondary fragments. Finally, the parameter Δ essentially represents the difference in the neutron-to-proton composition of the two sources considered in the isoscaling approach.

In this work, we investigated the isoscaling behavior of fragments with $Z = 1$–8. The fragments used in this study were fully isotopically resolved and originated from quasiprojectiles. The latter were selected from the reconstructed events using the criteria described in the previous

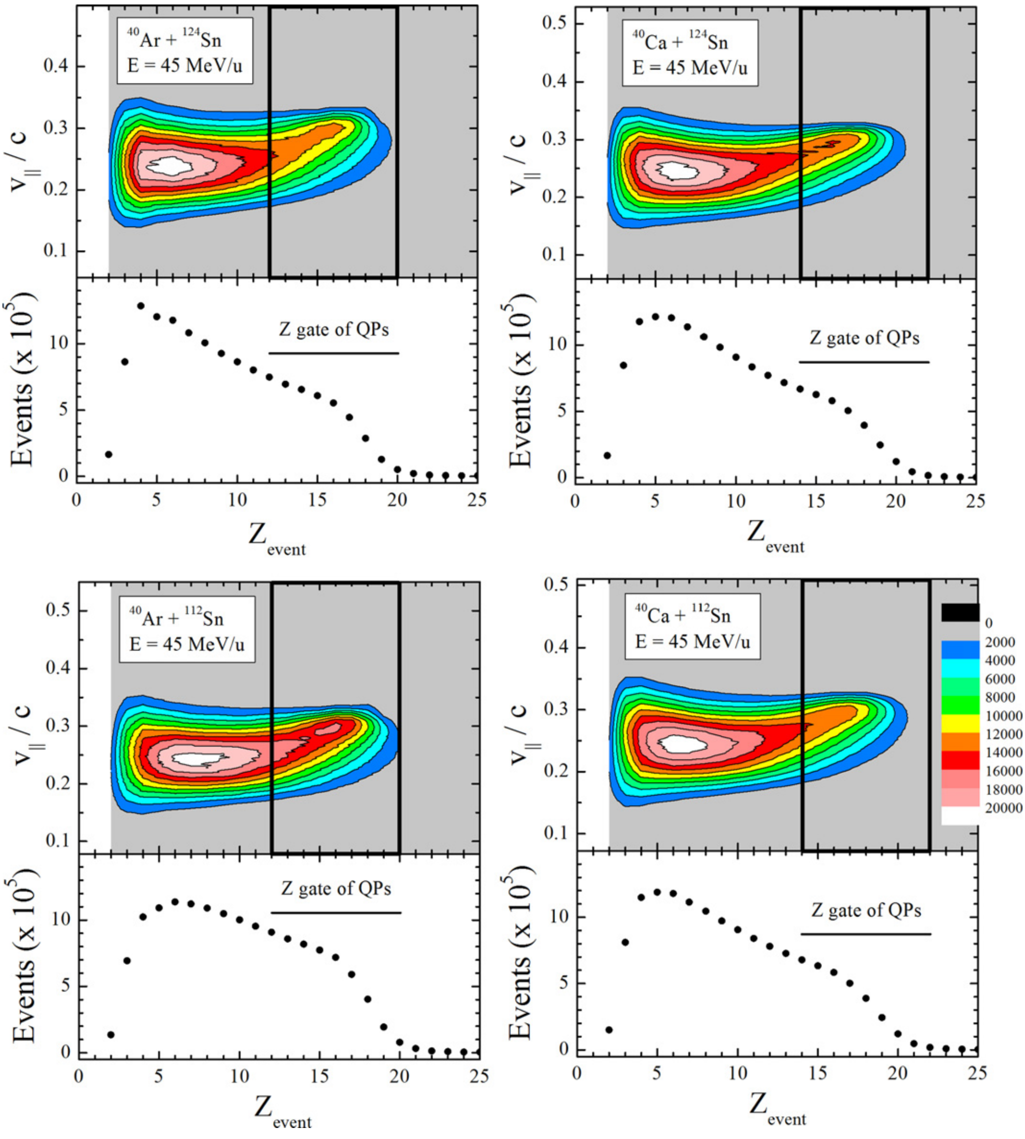

Fig. 2. (Color online.) Distributions of $\upsilon_{\parallel}/c$ versus Z_{event} (upper part of each panel) and Z_{event} distributions (lower part of each panel) of reconstructed events from the reactions ^{40}Ar + ^{124}Sn, ^{112}Sn and ^{40}Ca + ^{124}Sn, ^{112}Sn at beam energy of 45 MeV/nucleon. The velocity of the projectiles is $\upsilon_p = 0.31$c, whereas the velocity of the c.m. is approximately $\upsilon_{cm} = 0.07$c. The range of atomic numbers Z_{QP} of reconstructed quasiprojectiles is indicated with a box (upper parts) and a line (lower parts) in each panel.

section. Two sets of reaction pairs were employed in the isoscaling: first the ^{40}Ar + ^{124}Sn and ^{40}Ar + ^{112}Sn systems, and second the ^{40}Ca + ^{124}Sn and ^{40}Ca + ^{112}Sn ones. (As previously mentioned all reactions have been performed at the beam energy of 45 MeV/nucleon.) The “global” isoscaling (without quasiprojectile excitation energy selection – see below) obtained from these reaction pairs is displayed in the left and right panels of Fig. 3. As we can see, the quality of the

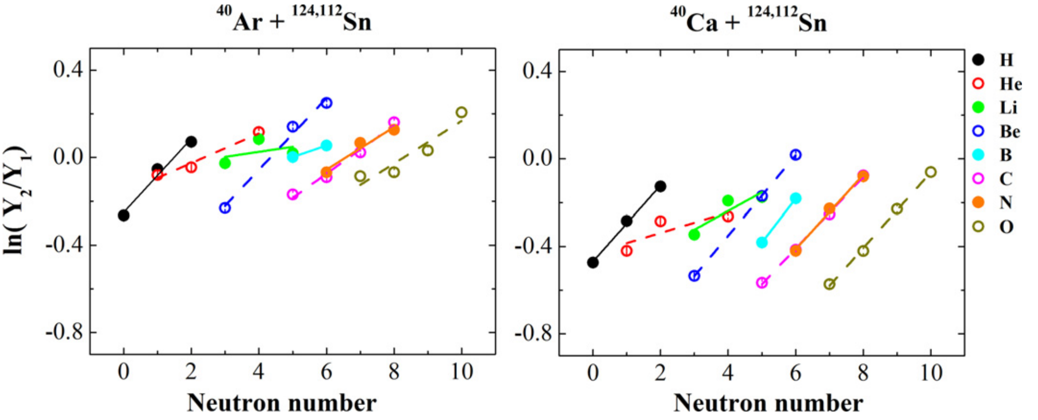

Fig. 3. (Color online.) Global isoscaling of fragments with $Z = 1–8$ from the reaction pairs $^{40}Ar + {}^{124}Sn$ versus $^{40}Ar + {}^{112}Sn$ (left panel) and $^{40}Ca + {}^{124}Sn$ versus $^{40}Ca + {}^{112}Sn$ (right panel).

isoscaling, in the sense of parallel and equidistant lines in the semilogarithmic plot (presenting the logarithm of the fragment yield ratio of a given element as a function of the neutron number) is not good.

Subsequently, we proceeded in performing cuts in the excitation energies of the quasi-projectiles. We defined 8 excitation energy bins from 1.5 to 8.5 MeV/nucleon with an energy width of 1 MeV. For each excitation energy bin, the behavior of the isoscaling was also investigated and the results are summarized in Fig. 4. Despite the restriction in the excitation energy of the sources, we did not observe a major improvement in the isoscaling behavior.

At this point we wish to point out that, in regards to the particle identification, the $\Delta E–E$ spectra are sufficiently clean for most of the isotopes [28]. However, a possible contribution from neighboring high-intensity isotopes and/or background cannot be excluded especially in the case of low yield isotopes such as He-3, He-6 and O-15, which may be responsible, in part, for the irregular behavior observed in Figs. 3 and 4. Nevertheless, as it will be shown in the following, the placement of gates in the N/Z parameter of the reconstructed quasiprojectile source makes it possible to "clean up" the spectra so that a regular isoscaling behavior emerges in all cases and can be followed as a function of the excitation energy of the quasiprojectile.

Following the conclusions and experience of our recent work [29,30] (corroborated by our previous work on a lighter system [31]), we infer that the main reason for the failure of isoscaling, as discussed above, is the rather broad distribution of the neutron to proton ratios $(N/Z)_{QP}$ of the quasiprojectiles from the neutron rich and the neutron deficient sources (even with the excitation energy selection criterion imposed). This becomes obvious in Fig. 5, where the distribution of the $(N/Z)_{QP}$ of the quasiprojectiles is presented. Indeed, for each reaction system, a broad range of N/Z of the fragmenting source is observed which contributes to the yield scaling.

In order to improve the isoscaling behavior, as shown in [29,30], our approach was to perform the isoscaling for each system separately using as sources a neutron-rich and a neutron-poor N/Z zone with sufficient statistics. The $(N/Z)_{QP}$ zones chosen for the $^{40}Ar + {}^{124}Sn$, ^{112}Sn reactions were 1.05–1.09 (neutron rich) and 0.91–0.95 (neutron poor). The corresponding zones for the $^{40}Ca + {}^{124}Sn$, ^{112}Sn reactions were 1.04–1.08 (neutron rich) and 0.92–0.96 (neutron poor). A linear correlation of the isoscaling parameter α with respect to Δ was observed in our previous work [30]. Thus, the choice of the N/Z zones is simply based on available statistics and an attempt to obtain a relatively large value of the isoscaling parameter α. From the mean N/Z

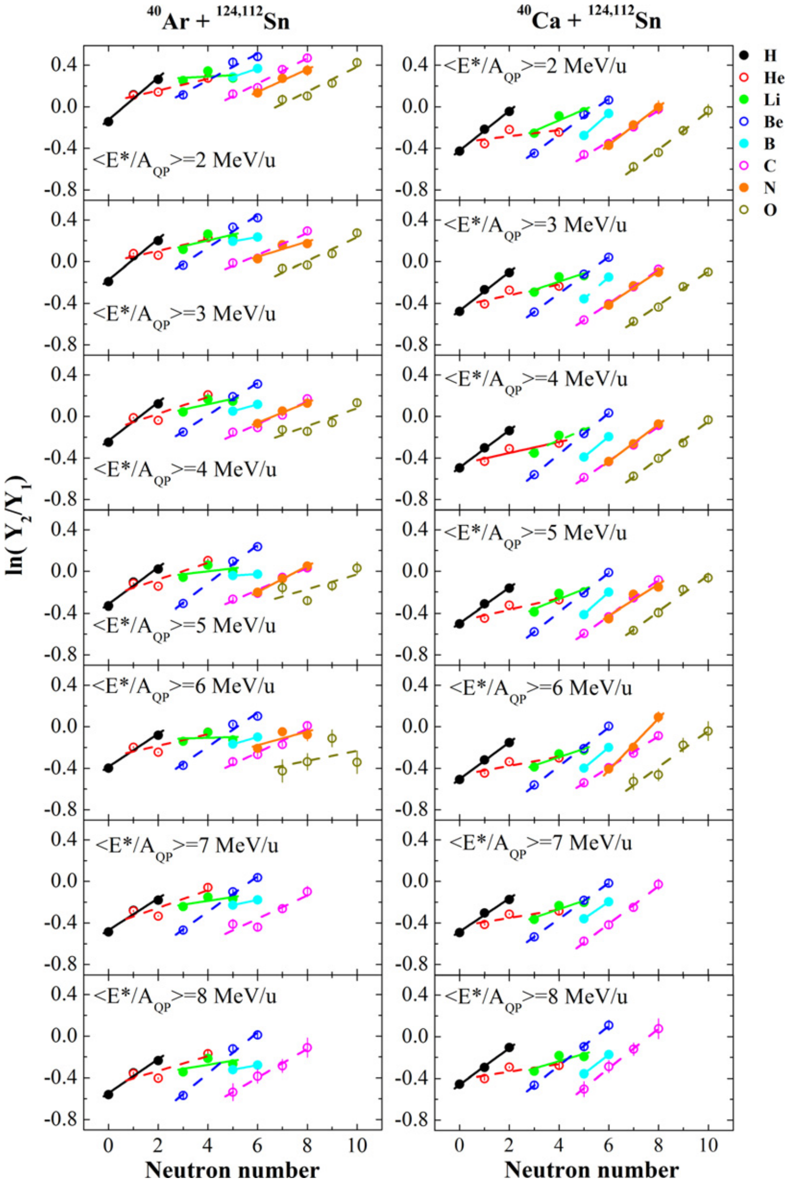

Fig. 4. (Color online.) Isoscaling of fragments with $Z = 1$–8 from the reaction pairs ^{40}Ar + ^{124}Sn, ^{112}Sn (left panel) and ^{40}Ca + ^{124}Sn, ^{112}Sn (right panel) performed for each of the indicated quasiprojectile excitation energy bins (see text).

values of the two N/Z zones for each of the four systems, the values of the Z/A of the sources were calculated and summarized in Table 1 along with the difference Δ in $(Z/A)^2$, following the definition in Eq. (5).

Employing the yields of the fragments from the two quasiprojectile sources for each system, the "intra-system" isoscaling behavior was studied in detail. In Fig. 6, the yield ratios of the

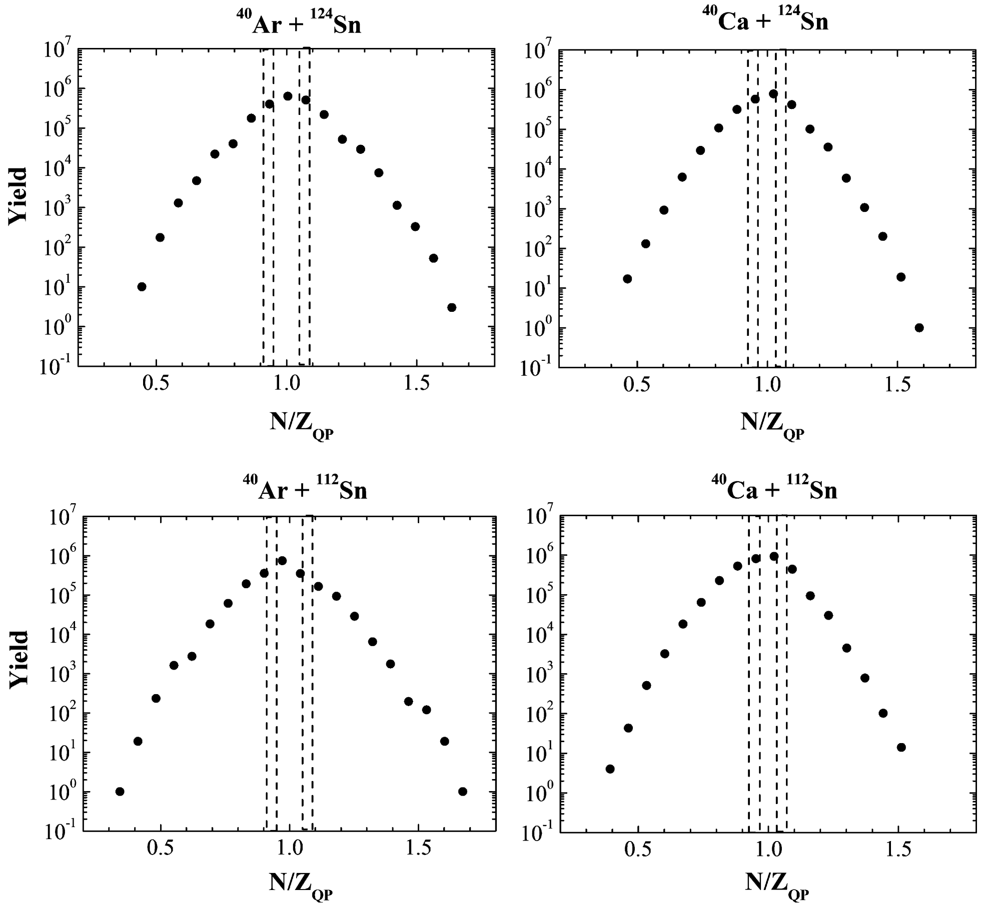

Fig. 5. Distributions of N/Z of the reconstructed quasiprojectiles for each reaction system studied in this work. In each panel, the dashed lines indicate the two narrow $(N/Z)_{QP}$ zones employed in the isoscaling procedure (see text).

Table 1
Values of quasiprojectile source Z/A and Δ for the four systems studied in this work. The neutron corrected values of Z/A and Δ are also given, along with the ratio of between the uncorrected to the uncorrected Δ (see text).

System	$(Z/A)_1$	$(Z/A)_2$	Δ	$(Z/A)_{1,corr}$	$(Z/A)_{2,corr}$	Δ_{corr}	$\frac{\Delta}{\Delta_{corr}}$
^{40}Ar + ^{124}Sn	0.518	0.483	0.035	0.502	0.442	0.056	0.62
^{40}Ar + ^{112}Sn	0.518	0.483	0.035	0.498	0.441	0.054	0.64
^{40}Ca + ^{124}Sn	0.516	0.485	0.031	0.498	0.441	0.053	0.58
^{40}Ca + ^{112}Sn	0.516	0.485	0.031	0.499	0.439	0.056	0.55

fragments from the above mentioned neutron rich and neutron poor quasiprojectile sources are presented for the four systems studied. The yield ratios of the fragments of the same element as a function of the neutron number can be fit by a straight line the slope of which gives the isoscaling parameter α (see Eq. (1)). As shown in Fig. 6, the fit lines are parallel and equidistant in the semilogarithmic plot, indicating a good isoscaling behavior. For completeness, we report

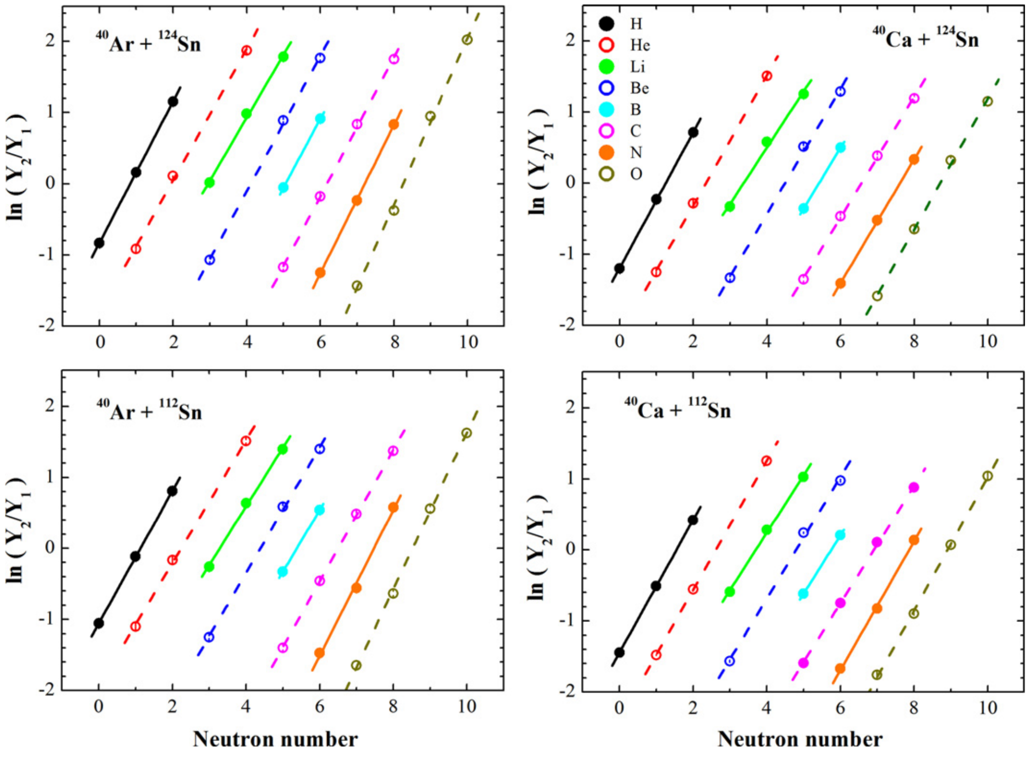

Fig. 6. (Color online.) Isoscaling of fragments from each of the indicated four systems using the neutron rich and the neutron deficient quasiprojectile N/Z zones of 1.05–1.09 and 0.91–0.95, respectively, for ^{40}Ar + ^{124}Sn, ^{112}Sn systems, and 1.04–1.08 and 0.92–0.96, respectively, for ^{40}Ca + ^{124}Sn, ^{112}Sn systems (see text). The average isoscaling parameters α (w.r.t. the elements $Z = 1$–8) for each of these systems are reported in the text.

the average isoscaling parameters α (w.r.t. the elements $Z = 1$–8) for each of these four systems which are, respectively, 1.00 ± 0.12, 0.96 ± 0.11, 0.87 ± 0.10 and 0.85 ± 0.10 (following the caption of Fig. 6).

Thus, the specification of narrow N/Z zones for the two quasiprojectile sources plays an important role in the isoscaling behavior. This can also be confirmed from the flattening of the isoscaling behavior, when yield ratios of fragments from only one N/Z quasiprojectile zone are taken from a pair of reactions as in ^{40}Ar + ^{124}Sn, ^{112}Sn displayed in Fig. 7. In this figure, the yield ratios for each element are obtained with the requirement that the quasiprojectile N/Z be 1.05–1.09. For each element, the yield ratio becomes nearly independent of the neutron number and, thus, the isoscaling behaviour becomes flat, as also indicated by the corresponding value of the average (over the elements $Z = 1$–8) isoscaling parameter $\alpha = 0.12 \pm 0.10$).

As a next step, the isoscaling for each of the above mentioned four reactions using the two N/Z zones is performed at each of the eight excitation energy bins. Again, at each excitation energy bin, the yield ratios of the fragments of the same element can be fit by straight lines whose slopes provide the isoscaling parameter α. As can be seen in Figs. 8 and 9, the fit lines are parallel and equidistant in the semilogarithmic plots, indicating an excellent isoscaling behavior. Moreover, as also shown in the upper panel of Fig. 11, the isoscaling parameter α determined for each excitation energy bin is found to decrease with increasing excitation energy.

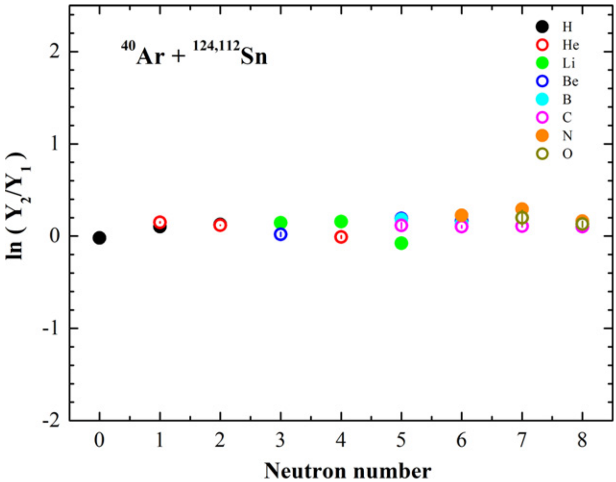

Fig. 7. (Color online.) Isoscaling of fragments from the pair of systems ^{40}Ar + ^{124}Sn, ^{112}Sn performed in reconstructed quasiprojectiles restricted in the region $N/Z = 1.05$–1.09. The isoscaling behaviour flattens out, as also indicated by the value of the average isoscaling parameter $\alpha = 0.12 \pm 0.10$ (see text).

As already discussed, the isoscaling parameter α is related to the symmetry energy coefficient C_{sym} through Eq. (5) which is now written in the form

$$\frac{\alpha}{\Delta} = \frac{4C_{sym}}{T}. \tag{6}$$

The term α/Δ, which we call reduced isoscaling parameter, collects the information we get from the isoscaling analysis of the present work and will be determined at each quasiprojectile excitation energy as described in the following. First, the isoscaling parameter α was obtained at each excitation energy bin of each reaction as an average of the values of α of each element and is presented in the upper panel of Fig. 11. Second, the parameter Δ, expressing the difference in the isospin asymmetry of the two fragmenting sources, was determined from the average N/Z values of the neutron-rich and the neutron-poor quasiprojectile N/Z zones (see Table 1). As pointed out, the neutrons produced in the reactions could not be detected by the experimental setup. For this reason, Δ has to be corrected for neutron loss. This correction of Δ was performed employing the theoretical models DIT (Deep Inelastic Transfer) [32] and SMM (Statistical Multifragmentation Model) [33], along with the Faust filter software which takes into account the geometry of the setup and the energy thresholds of the detectors [28] used in the experiment. More specifically, for each reaction system, corrections on the experimental values of the N/Z of the sources were made in the region from 0.8 to 1.2 (represented by the horizontal axis in the plots in Fig. 10) with the procedure described in the following.

First, primary hot quasiprojectiles were generated by the DIT code, describing the dynamical stage of the projectile–target interaction, and subsequently were deexcited by the SMM code. The resulting secondary fragments were then passed through the Faust filter [28]. From the fragments obtained after the Faust filter, following exactly the same reconstruction procedure that was followed in the experimental data, reconstructed quasiprojectiles were generated.

In Fig. 10, depicted as full points are the correlations of the N/Z values obtained for these reconstructed quasiprojectiles (horizontal axis) versus the corresponding initial N/Z as obtained directly from the DIT code (vertical axis) for each of the four systems. This correlation, obtained

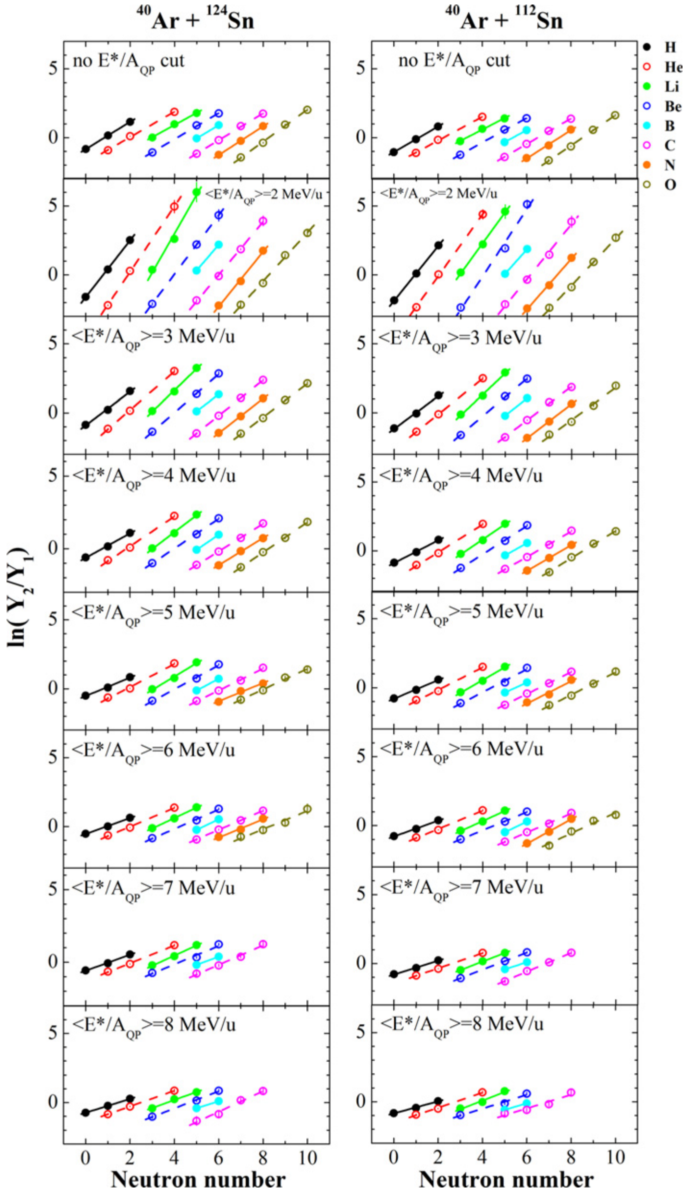

Fig. 8. (Color online.) Isotopic yield ratios of fragments from reconstructed sources (quasiprojectiles) for the ^{40}Ar + ^{124}Sn, ^{112}Sn reactions at 45 MeV/nucleon. The isoscaling is performed using fragments from the neutron-rich and neutron-deficient N/Z bins (see also Fig. 5) for the 8 excitation energy bins as described in the text. In the upper panels, the isoscaling without the excitation energy cuts (same as in Fig. 6) is repeated for comparison.

with the aid of the above simulation procedure, allows us to correct a given experimentally obtained value of $(N/Z)_{QP}$ (that has been affected by the neutron non-detection) and obtain the corresponding value $(N/Z)_{QP,corr}$ (in which the effect of the neutrons has been accounted for). To point out the effect of the neutron loss in the values of the quasiprojectile N/Z, in Fig. 10

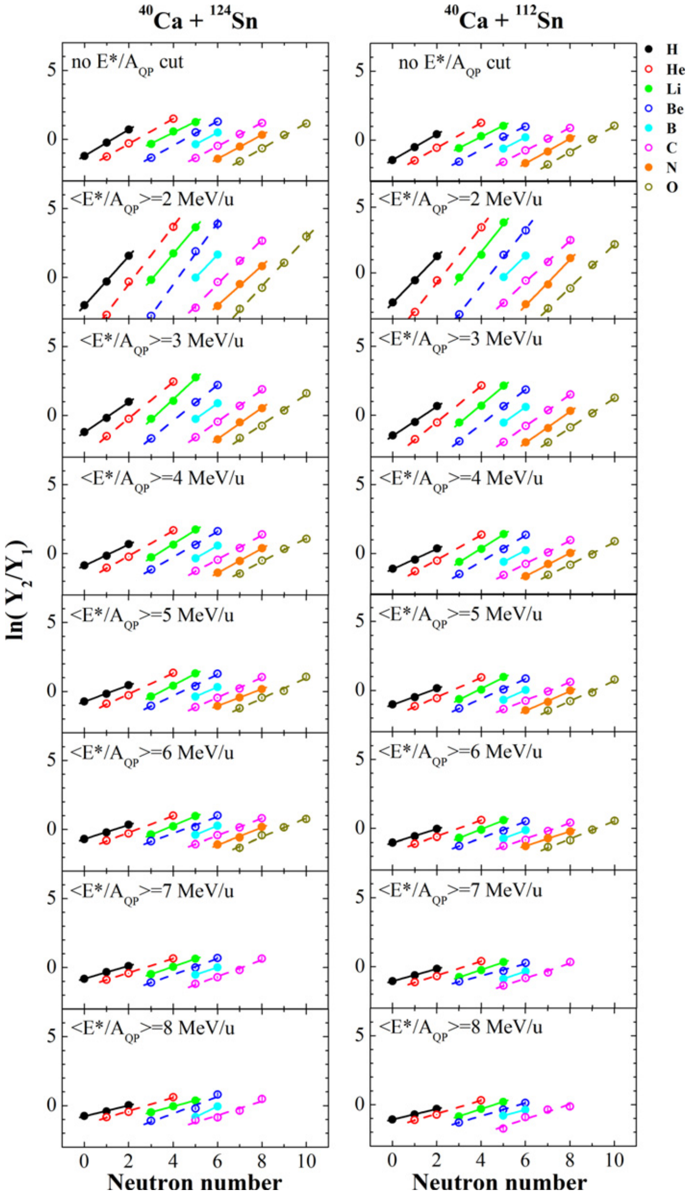

Fig. 9. (Color online.) Isotopic yield ratios of fragments from reconstructed sources (quasiprojectiles) for the ^{40}Ca + ^{124}Sn, ^{112}Sn reactions at 45 MeV/nucleon. The isoscaling is performed using fragments from the neutron-rich and neutron-deficient N/Z bins (see also Fig. 5) for the 8 excitation energy bins as described in the text. In the upper panels, the isoscaling without the excitation energy cuts (same as in Fig. 6) is repeated for comparison.

we present as dashed lines the correlations of the N/Z of quasiprojectiles in the case that no neutron loss was present [28]. As expected, the effect of the neutron loss is more important in the correction of the N/Z of the neutron-rich quasiprojectiles than in the N/Z of the neutron deficient ones. To get corrections at any value of the N/Z ratio, second order polynomials were

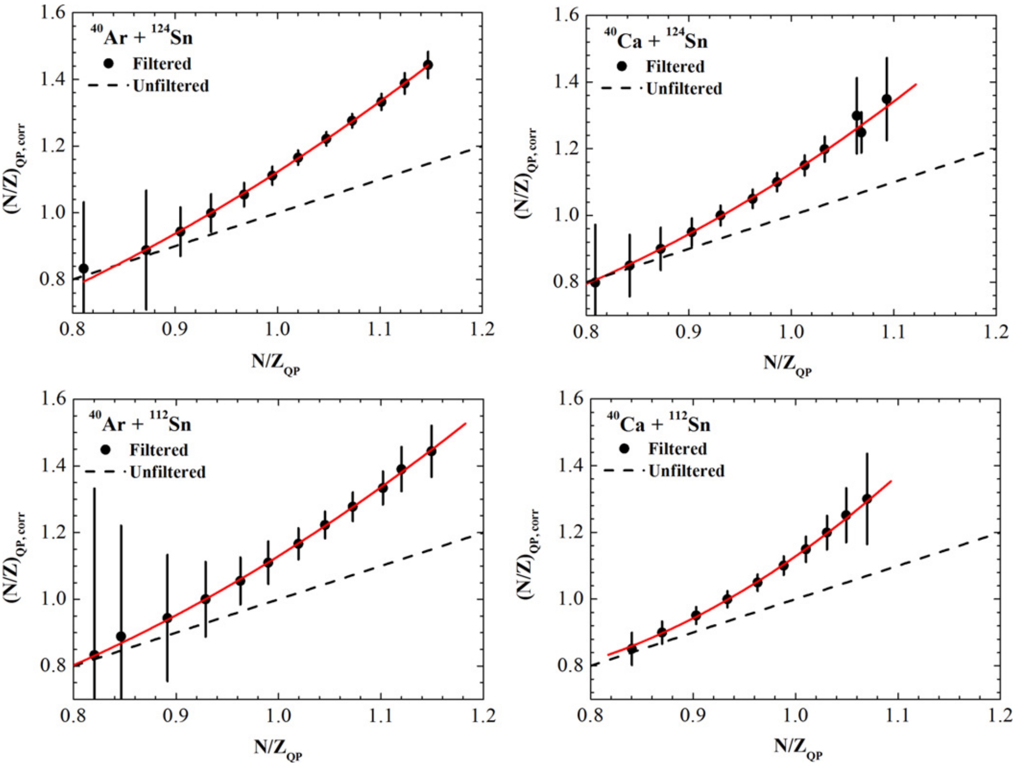

Fig. 10. (Color online.) Solid points: correlations of the N/Z of reconstructed quasiprojectiles (horizontal axis) following the DIT/SMM/filter simulation procedure versus the corresponding initial N/Z obtained directly from the DIT code (vertical axis). The former values reflect the effect of the neutron loss, whereas the latter values correspond to no neutron loss (see text). Solid lines: second order polynomial fits corresponding to the solid points. Dashed lines: correlations of the N/Z of quasiprojectiles in the case that no neutron loss is present [28] (see text).

fit, as shown by the solid lines on the four panels of Fig. 10. We note that the average correlations depicted in Fig. 10 are very similar for the four systems. We point out that they have been obtained using the whole ensemble of events from the DIT/SMM/filter simulation without any cut in the excitation energy of the quasiprojectiles.

After the aforementioned correction procedure for N/Z, corrected values of Δ were obtained and summarized in Table 1. Comparing the values of the uncorrected and corrected Δ, we observe a substantial decrease in Δ ($\sim 40\%$) due to the effect of the neutron loss. This difference emphasizes the importance of the correction in the determination of Δ when it is meant to be used in Eq. (5) (or Eq. (6)) to probe the nuclear symmetry energy.

Using the corrected Δ values along with the isoscaling parameters α, the corrected reduced isoscaling parameter α/Δ was determined at each excitation energy bin. (We note that the QP excitation energy per nucleon has not been corrected for neutron loss of the QP sources. We expect this correction in the excitation energy to be relatively small.)

The values of the corrected α/Δ as a function of the quasiprojectile excitation energy for each system are shown in the lower panel of Fig. 11. Given the dependence of α on excitation energy (upper panel of Fig. 11), the reduced isoscaling parameter α/Δ, of course, decreases with increasing excitation energy for each system. At each excitation energy bin, the average

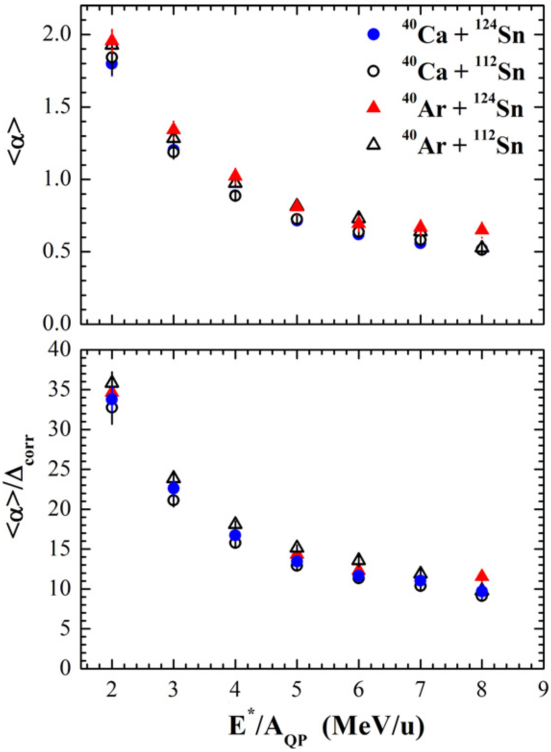

Fig. 11. (Color Online.) Upper panel. Isoscaling parameter α as a function of the excitation energy of the fragmenting sources for the four systems studied in this work. Lower panel. As in the upper panel, but presenting the reduced isoscaling parameter α/Δ as a function of the excitation energy (see text).

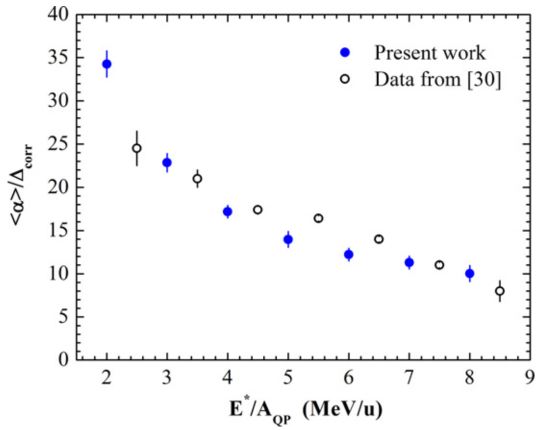

Fig. 12. (Color Online.) Dependence of the average value of the reduced isoscaling parameter α/Δ on quasiprojectile excitation energy for the systems of the present work (solid points) and comparison with the corresponding data (open points) from [30] (see text).

values of α/Δ for the four systems were obtained and are shown by the full points in Fig. 12. Also shown in this figure are the values of α/Δ obtained in our recent work [30] on mass A $\simeq$ 80 reconstructed quasiprojectiles. We point out that the N/Z correction procedure followed in [30] was based on measured neutron multiplicities [34], whereas in the present work it was performed via the DIT/SMM/filter simulation procedure. We observe that the two sets of data are in good agreement, despite the mass difference of the sources (i.e., mass A $\simeq$ 40 in the present work and mass A $\simeq$ 80 in [30]) and the neutron correction procedure for the quasiprojectile source N/Z used in the isoscaling procedure. In addition, the fair comparison between the two data sets provides confidence in the neutron loss correction approach followed in the present work.

4. Discussion and future directions

The consistent decrease of the reduced isoscaling parameter α/Δ with excitation energy obtained in the present work, as well as in [30] may be connected to a decrease of the symmetry energy coefficient with increasing excitation energy. In the following we summarize the arguments and related recent work that support this conclusion.

First, as observed in our work [30] in which the isoscaling was extended from $Z = 1$ up to $Z = 17$, no dependence of the isoscaling parameter on the fragment Z was observed. (The same is true in the limited range of $Z = 1$–8 of the present work.) Consequently, there seems to be no experimental evidence for a significant surface dependence of the symmetry energy. Such a dependence would, in turn, lead to a dependence of the isoscaling parameter α on the fragment Z as suggested in [23,35]. Second, it was pointed out in [30] that the expected change in temperature (from approximately 5.5 to 7.0 MeV) in the E^*/A range 2.5–8.5 MeV can account for no more than about 15% of the decrease of the parameter α/Δ for the mass A $\simeq$ 80 systems studied. Furthermore, in the E^*/A range of 2.5–4.5 MeV, under the scenario of sequential emission of a source at normal density, it was shown that the overall decrease in α/Δ could be again no more than approximately 15%. This conclusion is also supported by the isoscaling studies performed by Tian et al. [36] employing the sequential decay code GEMINI [37].

In the same vein, the extended compound nucleus (ECN) model of Tõke et al. [25] (in its present implementation assuming emission from an equilibrated compound nucleus at normal density) implies that the symmetry energy C_{sym} is essentially independent of temperature. As stated by the authors of [25], the complete ECN model (that is currently under development) incorporating nuclear expansion with excitation is expected to provide a decreasing C_{sym} with increasing excitation as a result of nuclear expansion, i.e. decreasing density. Similar conclusions are extracted from the results of the mean-field calculations reported in [38] and also in [39]. Thus, we can summarize that a large part of the experimentally observed decrease of the parameter α/Δ with increasing excitation energy may be attributed to the ensuing decrease of the density due to nuclear expansion [40].

In order to extract absolute values of the nuclear symmetry energy, employing Eq. (5), experimental values of the temperature must be obtained (see, e.g., [31,34]). In addition, the effect of the secondary decay of the excited primary fragments on the experimentally obtained isoscaling parameter α should be investigated in detail (see, e.g., [41]). At this point, we remind the reader that Eq. (5), while first derived within a macrocanonical description of fragment formation [16,17], it has also been obtained within canonical and microcanonical approaches [16,21, 35], as well as dynamical approaches [23]. Despite possible limitations of Eq. (5) recently discussed in the literature (e.g. [24,35,42]), in the present work, we employ this simple expression to obtain information on the symmetry energy of the decaying source.

As a subsequent step towards the probing of the density dependence of the symmetry energy [2], an experimental determination of the source density at each excitation energy should be obtained (see, e.g., [40] and references therein). Such determination is essentially based on the assumption of a freeze-out stage characterized by a certain temperature and density. The asymptotic values of the kinetic energies of the fragments (that eventually reach the detectors) are related to the Coulomb energies of these fragments at the freeze-out stage and can thus provide information on the average density of this freeze-out configuration. Although the fragment emission may be sequential (including preequilibrium, as well as equilibrium emission), the freeze-out picture may remain valid within the limit of the short timescale of the multifragmentation process. The symmetry energy that can be obtained by the aforementioned procedure is thus directly related to the density at the freeze-out stage.

In regards to our experimental analysis approach, we wish to comment that, while we set gates on the E^*/A of the quasiprojectile source, the finite width (1 MeV) of these gates does not qualify our approach as microcanonical. It may, rather, be characterized as pseudo-microcanonical. For each E^*/A bin (characterized by its mean value), a temperature can be obtained via isotope thermometry which is the subject of ongoing work.

In addition, with respect to the meaning of the narrow N/Z gates that were indispensable for the clean isoscaling behavior obtained in our works, we wish to add the following comments. As follows from detailed analysis performed in the work [43], with the placement of the narrow N/Z gates for two hot sources, the resulting isoscaling behavior essentially decouples from the effect of the dynamical stage of the reaction which leads to the broad spectrum of N/Z (as shown in Fig. 5). This experimental elimination of the dynamical stage allows access into the details of the deexcitation stage, i.e., the statistical multifragmentation process. Thus, also the values of the extracted symmetry energy represent the behavior given by the nuclear EOS, without distortion caused by the reaction dynamics. We further stress that the isoscaling (and, thus, the isospin/symmetry energy) information on that stage can be obtained by only one reaction, provided that full reconstruction of the quasiprojectile is possible.

An alternative approach to extract the density dependence of the symmetry energy may be provided by the complete ECN model [25] (see discussion above). Within the extended compound nucleus picture, each E^*/A corresponds to a certain density of the expanded nucleus at which the fragments are formed. A comparison of the isoscaling predictions from ECN with the experimental results, as given in Fig. 12, can provide, within the ECN description, information on the density dependence of the symmetry energy.

Finally, apart from a statistical description of the isoscaling observations, fully dynamical calculations of fragment formation may be pursued, as, e.g., employing the N-body Constrained Molecular Dynamics (CoMD) model [44]. Comparisons of the experimental isoscaling data with such dynamical calculations are expected to provide constraints on the effective interactions employed in the model and thus shed light on the nuclear equation of state and, more specifically, the symmetry energy and its density dependence.

At present we are actively pursuing both the statistical and the dynamical approaches for the description of the experimental isoscaling data. We believe that detailed results from both approaches and comparisons between them may contribute to the advancement of our understanding of the nuclear symmetry energy in the range of excitation energies (and temperatures) at subsaturation densities corresponding to the multifragmentation process.

5. Summary

In this work, a systematic study of fragment isoscaling in reconstructed quasiprojectiles of mass A $\simeq 40$ obtained in peripheral collisions of ^{40}Ar + ^{124}Sn, ^{112}Sn and ^{40}Ca + ^{124}Sn, ^{112}Sn at 45 MeV/nucleon was presented. After initial efforts to obtain isoscaling with the "traditional" approach of using pairs of systems differing in their N/Z, "intra-system" isoscaling for each of the four systems was performed using as quasiprojectile sources two narrow N/Z regions (one neutron-rich and one neutron-poor). The observed isoscaling behavior was excellent and the isoscaling parameter α was found to decrease with increasing excitation energy. Correction for neutron loss of the N/Z of the sources was performed (based on DIT/SMM and the software filter of the detector) and was applied to the determination of the parameter Δ (expressing the difference in isospin asymmetry of the two sources used in the isoscaling). The reduced isoscaling parameter α/Δ was found to decrease as the excitation energy of the quasiprojectile source increases, in good agreement with the recent work on reconstructed mass A $\simeq 80$ quasiprojectiles [30]. This consistent decrease of α/Δ may indicate a possible decrease of the symmetry energy coefficient with increasing excitation energy.

Acknowledgements

We wish to thank A. Bonasera and R. Tripathi for fruitful discussions and suggestions. This work was supported in part by the Department of Energy, Grant Number: DE-FG02-93ER40773 and the Robert A. Welch Foundation, Grant Number A-1266. M.V. acknowledges support by the Slovak Scientific Grant Agency under contract VEGA-2/0073/08.

References

[1] B.A. Li, L.W. Chen, C.M. Ko, Phys. Rep. 464 (2008) 113.
[2] D.V. Shetty, S.J. Yennello, G.A. Souliotis, Phys. Rev. C 76 (2007) 024606.
[3] J.R. Stone, P.G. Reinhard, Prog. Part. Nucl. Phys. 58 (2007) 587.
[4] V. Baran, et al., Phys. Rep. 410 (2005) 335.
[5] A.W. Steiner, et al., Phys. Rep. 411 (2005) 325.
[6] J.M. Lattimer, M. Prakash, Phys. Rep. 333 (2000) 121.
[7] J.R. Stone, et al., Phys. Rev. C 68 (2003) 034324.
[8] A.S. Botvina, I.N. Mishustin, Phys. Lett. B 584 (2004) 233.
[9] K. Oyamatsu, et al., Nucl. Phys. A 634 (1998) 3.
[10] B.A. Brown, Phys. Rev. Lett. 85 (2000) 5296.
[11] C.J. Horowitz, J. Piekarewicz, Phys. Rev. Lett. 86 (2001) 5647.
[12] R.J. Furnstahl, Nucl. Phys. A 706 (2002) 85.
[13] D.T. Khoa, H.S. Than, Phys. Rev. C 71 (2005) 044601.
[14] L.W. Chen, C.M. Ko, B.A. Li, Phys. Rev. Lett. 94 (2005) 032701.
[15] Y. Zhang, Z. Li, Phys. Rev. C 71 (2005) 024604.
[16] M.B. Tsang, et al., Phys. Rev. Lett. 86 (2001) 5023;
M.B. Tsang, et al., Phys. Rev. C 64 (2001) 054615.
[17] A.S. Botvina, O.V. Lozhkin, W. Trautmann, Phys. Rev. C 65 (2002) 044610.
[18] M. Colonna, M.B. Tsang, Eur. Phys. J. A 30 (2006) 165.
[19] G.A. Souliotis, et al., Phys. Rev. C 68 (2003) 024605.
[20] G.A. Souliotis, et al., Phys. Rev. C 73 (2006) 024606.
[21] G. Chaudhouri, S. Das Gupta, M. Mocko, Nucl. Phys. A 813 (2008) 293.
[22] S.R. Souza, et al., Phys. Rev. C 78 (2008) 014605.
[23] A. Ono, et al., Phys. Rev. C 68 (2003) 051601.
[24] G. Lehaut, F. Gulminelli, O. Lopez, Phys. Rev. Lett. 102 (2009) 142503.

[25] W. Ye, J. Tõke, W.U. Schröder, Phys. Lett. B 676 (2009) 193.
[26] F. Gimeno-Nogues, et al., Nucl. Instr. Meth. A 399 (1997) 94.
[27] D. Rowland, et al., Phys. Rev. C 67 (2003) 064602.
[28] A.L. Keksis, Ph.D. thesis, Cyclotron Institute, Texas A&M University, 2007.
[29] S. Galanopoulos, et al., AIP Conf. Proc. 1099 (2009) 786.
[30] S. Wuenschel, et al., Phys. Rev. C 79 (2009) 061602.
[31] M. Veselsky, G.A. Souliotis, S.J. Yennello, Phys. Rev. C 69 (2004) 031602.
[32] L. Tassan-Got, C. Stéphan, Nucl. Phys. A 524 (1991) 121.
[33] A.S. Botvina, et al., Nucl. Phys. A 475 (1987) 663.
[34] S. Wuenschel, Ph.D. thesis, Cyclotron Institute, Texas A&M University, 2009.
[35] Ad.R. Raduta, F. Gulminelli, Phys. Rev. C 75 (2007) 024605.
[36] W.D. Tian, et al., Phys. Rev. C 76 (2007) 024607.
[37] R.J. Charity, et al., Nucl. Phys. A 483 (1988) 371.
[38] J. Xu, L.W. Chen, B.A. Li, H.R. Ma, Phys. Rev. C 75 (2007) 014607.
[39] S.K. Samaddar, J.N. De, X. Viñas, M. Centelles, Phys. Rev. C 76 (2007) 041602.
[40] D.V. Shetty, et al., J. Phys. G 36 (2009) 075103.
[41] D.V. Shetty, et al., Phys. Rev. C 71 (2005) 024602.
[42] S.R. Souza, et al., Phys. Rev. C 80 (2009) 041602.
[43] M. Veselsky, Phys. Rev. C 74 (2006) 054611.
[44] M. Papa, T. Maruyama, A. Bonasera, Phys. Rev. C 64 (2001) 024612.